
Vectorial Padé approximants in the Asymptotic Numerical Method

Noureddine Damil — Rédouane Jamai — Hassane Lahmam

*Laboratoire de Calcul Scientifique en Mécanique,
Faculté des Sciences Ben M'Sik
Université Hassan II - Mohammedia
Avenue Cdt Driss El Harti, BP 7955, Casablanca, MAROC
n.damil@univh2m.ac.ma, h.lahmam@univh2m.ac.ma*

ABSTRACT. In this paper, we present and discuss some techniques to define vectorial Padé approximants and quadratic approximants in the Asymptotic Numerical Method (ANM). For this purpose we have to orthonormalize the basis generated by the ANM. We shall discuss the influence of the orthonormalization procedure. We give some numerical comparisons of these techniques on non-linear elastic shells problems.

RÉSUMÉ. Dans cet article, nous présentons et discutons quelques techniques pour définir des approximants de Padé vectoriels et des approximants quadratiques dans la Méthode Asymptotique Numérique (MAN). La définition de ces approximants passe par une orthonormalisation de la base générée par la MAN. Nous discuterons l'influence de la procédure d'orthonormalisation. Des comparaisons numériques de ces techniques seront illustrées sur des problèmes de coques élastiques non linéaires.

KEYWORDS: vectorial Padé approximants, asymptotic numerical method, quadratic approximants, non-linear elastic shells.

MOTS-CLÉS : approximants de Padé vectoriels, méthode asymptotique numérique, approximants quadratiques, coques élastiques non linéaires.

1. Introduction

The vectorial Padé approximants were introduced in the Asymptotic Numerical Method (ANM) to improve the domain of validity of vectorial series (the polynomial) representation [COC 94a]. In the ANM, the polynomial representation of the solution path (U, λ) of a non-linear problem:

$$R(U, \lambda) = 0 \quad [1]$$

is a parametric representation in the form of integro-power series of vectors [DAM 90], [COC 94b]:

$$U(a) \simeq U_{pol(p)}(a) = U_0 + aU_1 + a^2U_2 + \cdots + a^pU_p \quad [2]$$

where p is an arbitrary order of truncature, U_0 is a given solution of the non-linear problem [1] and a is a path parameter (displacement parameter, load parameter or arc-length parameter). By introducing [2] in [1], the vectors fields $(U_i)_{1 \leq i \leq p}$ are the solutions of a recurrent sequence of linear problems, with a single tangent operator L_t to be inverted:

$$R_0 + aR_1 + a^2R_2 + \cdots = 0 \quad [3]$$

$$R_i = 0 \iff L_t U_i = F_i^{nl} \quad [4]$$

These linear problems [4], where F_i^{nl} are the right hand sides which depend on the previously computed vectors U_i , are generally solved by the finite element method. Of course, the domain of validity of the representation [2] is limited by the radius of convergence of the series. So the range of validity defines one step of the solution path. To obtain the entire solution path, a continuation procedure consists to repeat the ANM from the last point of the domain of validity to the previous step [COC 94a], [COC 94c], [COC 94b].

In order to extend the domain of validity of the representation [2] and to reduce the number of steps needed to obtain the entire solution path, in [COC 94a], a rational approximation, called Padé approximant [PAD 92], [VAN 84], [BRE 94], [BAK 96], has been used.

By definition ([PAD 92], [BAK 96]), the scalar Padé approximant $f[L, M](a)$ of a scalar series, $f(a) = \sum f_k a^k$, is a rational fraction:

$$f[L, M](a) = \frac{A_0 + A_1 a + \cdots + A_L a^L}{1 + B_1 a + \cdots + B_M a^M} \quad [5]$$

having the same $(L + M)$ first coefficients of Mac-Laurin expansion as the scalar function $f(a)$. These ordinary Padé approximants [5] are defined as a solution of the linear equation:

$$-A(a) + B(a)f[L, M](a) = 0 \quad [6]$$

where the polynomials A and B have respectively the degrees L and M and satisfy the relation:

$$-A(a) + B(a)f(a) = O(a^{L+M+1}) \quad [7]$$

There are other techniques to improve the series, as the quadratic approximants [SHA 74]:

$$f[L, M, N](a) = \frac{-B(a) \pm \sqrt{B^2(a) - A(a)C(a)}}{C(a)} \quad [8]$$

which are a generalization of Padé approximants. Quadratic approximants $f[L, M, N]$ of a series f are defined as a solution of the quadratic equation:

$$A(a) + 2B(a)f[L, M, N](a) + C(a)f^2[L, M, N](a) = 0 \quad [9]$$

where the polynomials A , B and C have respectively the degrees L , M and N and satisfy the relation :

$$A(a) + 2B(a)f(a) + C(a)f^2(a) = O(a^{L+M+N+2}) \quad [10]$$

In [COC 94a], the representation [2] has been rewritten in an orthonormal basis built up from the basis (U_i) generated by the ANM and a strategy to use vectorial Padé approximants has been applied. This has been used in various fields [AZR 92], [TRI 96], [DEB 97]. But this strategy had the disadvantage to generate a great number of poles inside the domain of validity. An alternative, presented in [BRA 97], [NAJ 98], is to use vectorial Padé approximants with a common denominator, called simultaneous Padé approximants [BRE 94], [BAK 96].

Many applications in structural mechanics (for instance non-linear elasticity and contact), [COC 94b], [BRA 95], [NAJ 96], [BRA 97], [NAJ 98], [ELH 98], [ZAH 98], see more references in the ANM articles of this special issue, have established that vectorial Padé approximants with a common denominator can reduce the number of poles and permit to obtain more regular solutions. By using this rational representation in a continuation procedure, the number of steps to obtain the entire solution path has been reduced [ELH 00]. The vectorial Padé approximants have also been considered to accelerate the convergence of high order iterative algorithms for linear [CAD 01] or non-linear [DAM 99], [MAL 99], [LAH 02], [JAMA 02] problems.

The aim of this paper is to discuss some techniques to define vectorial Padé approximants and vectorial quadratic approximants in the the framework of the ANM and to show that their utilisation can improve clearly the vectorial polynomial representation.

In the second part, we remind the basis of the classical rational representation using the Padé approximants with a common denominator and we propose an improvement using all the vectors generated by the ANM. In this part, we propose also another method to built up a basis from the ordinary basis generated by the ANM which permits to define new vectorial Padé approximants without orthonormalizing the whole basis (U_i) . All the approximations are applied on some examples from non-linear elastic shells which are presented and analysed in the third part. In the fourth part, we discuss the influence of the Gram-Schmidt algorithms and the scalar product [JAM 03] on the quality of the solution. In the last part we propose some techniques to define vectorial quadratic approximants in the ANM [JAM 01], [JAM 02].

2. Rational representations

2.1. The classical rational representation used in the ANM

In order to define scalar Padé approximant [5], we first orthonormalize the basis U_1, \dots, U_p . The Gram-Schmidt procedure is the most known method in linear algebra, to compute an orthonormal basis U_1^*, \dots, U_p^* from the space generated by the vectors U_1, \dots, U_p in the following manner:

$$\begin{aligned} \alpha_{1,1}U_1^* &= U_1 \\ \alpha_{i,i}U_i^* &= U_i - \sum_{j=1}^{i-1} \alpha_{i,j}U_j^* \\ \langle U_i^*, U_j^* \rangle &= \delta_{i,j} \quad (i, j = 1, \dots, p). \end{aligned} \quad [11]$$

The Gram-Schmidt procedure permits also the computation of the scalar coefficients $\alpha_{i,j}$ called Gram-Schmidt coefficients. If we rewrite the representation [2] in the orthonormal basis (U_i^*) , we obtain exactly:

$$U_{pol(p)}(a) = U_0 + af^1(a)U_1^* + a^2f^2(a)U_2^* + \dots + a^p f^p(a)U_p^* \quad [12]$$

where f^i are scalar series defined by: $f^i(a) = \sum_{k=0}^{p-i} \alpha_{i+k,i} a^k$. In a previous work [COC 94b], the scalar series f^i has been replaced by some scalar Padé approximants $f^i[L^i, M^i]$ but this technique generated a lot of poles inside the domain of validity.

To avoid this drawback, rational fractions with a common polynomial, called also simultaneous Padé approximants [BRE 94], [BAK 96], have been introduced. Within the classical rational representation used in the ANM, the polynomial representation [12] is truncated at the order $q = p - 1$, and then the scalar series f^i are replaced by rational fractions $f^i[p - i - 1, p - 1] = \frac{A^i}{B}$ having the same denominator B [NAJ 98]. After some rearrangement, the following vectorial Padé representation [NAJ 98] of the solution is obtained:

$$U_{pad(p)}(a) = U_0 + a \frac{\Delta_{p-2}}{\Delta_{p-1}} U_1 + \dots + a^{p-2} \frac{\Delta_1}{\Delta_{p-1}} U_{p-2} + a^{p-1} \frac{1}{\Delta_{p-1}} U_{p-1} \quad [13]$$

where Δ_i are polynomials defined by:

$$\Delta_i(a) = 1 + B_1 a + B_2 a^2 + \dots + B_i a^i \quad [14]$$

The $p - 1$ coefficients $(B_i)_{i=1}^{p-1}$ of the polynomial Δ_i ($B = \Delta_{p-1}$) are computed from the following relations:

$$B_i = -\frac{1}{\alpha_{p-i,p-i}} \left(\alpha_{p,p-i} + \sum_{k=1}^{i-1} B_k \alpha_{p-k,p-i} \right) \quad [15]$$

For problems depending on a parameter λ , as path following in structural mechanics (for instance in non-linear elasticity problems or contact problems, λ represents a load parameter), the polynomial representation of the parameter λ :

$$\lambda(a) \simeq \lambda_{pol(p)} = \lambda_0 + a\lambda_1 + \dots + a^{p-1}\lambda_{p-1} + a^p\lambda_p \quad [16]$$

is also replaced by a Padé approximant $\lambda[p-1, p-1] = \frac{A^\lambda}{B}$ having the same denominator B as the Padé approximants $f^i[p-i-1, p-1]$. After some rearrangement a rational representation analogous to [13] is obtained:

$$\lambda_{pad(p)}(a) = \lambda_0 + a \frac{\Delta_{p-2}}{\Delta_{p-1}} \lambda_1 + \cdots + a^{p-2} \frac{\Delta_1}{\Delta_{p-1}} \lambda_{p-2} + a^{p-1} \frac{1}{\Delta_{p-1}} \lambda_{p-1} \quad [17]$$

2.2. An improvement of this classical rational representation

To get the rational representation [13], [17], the polynomial representation [12] has been truncated at the order $q = p - 1$ before using Padé approximants. So, the last term $a^p f^p U_p^*$ in [12] was not used in the previous rational representation. Now, we propose to avoid this truncation and to keep all the vectors in the polynomial representation [12].

We approximate the first $p - 1$ polynomials f^i by the Padé approximants $f^i[p - i - 1, p - 1] = \frac{A^i}{B}$ for $i = 1, \dots, p - 1$ as it was done in the previous part. The last polynomial f^p is approximated by the Padé approximant $f^p[0, p - 1] = \frac{A_p}{B}$ ($A_p = \alpha_{p,p}$) and the parameter λ is approximated by the rational fraction $\lambda[p, p - 1] = \frac{A^\lambda}{B}$.

If we return to the basis U_i , we obtain after some rearrangement, [JAM 02], a new vectorial Padé representation:

$$\begin{aligned} U_{npad(p)}(a) &= U_0 + a \frac{\Delta_{p-1}}{\Delta_{p-1}} U_1 + \cdots + a^{p-1} \frac{\Delta_1}{\Delta_{p-1}} U_{p-1} + a^p \frac{1}{\Delta_{p-1}} U_p \\ \lambda_{npad(p)}(a) &= \lambda_0 + a \frac{\Delta_{p-1}}{\Delta_{p-1}} \lambda_1 + \cdots + a^{p-2} \frac{\Delta_1}{\Delta_{p-1}} \lambda_{p-1} + a^p \frac{1}{\Delta_{p-1}} \lambda_p \end{aligned} \quad [18]$$

As compared with the classical vectorial Padé representation [13], [17], the fractions $\frac{\Delta_i}{\Delta_{p-1}}$ are shifted in the new rational representation [18] one degree forward and the last vector U_p appears in the representation [18].

2.3. Another method to define Padé approximants in the ANM

Previously the Gram-Schmidt orthonormalization procedure has been used to rewrite the polynomial representation [2] in an orthonormal basis in order to obtain scalar series that we replace by a Padé approximation. To minimize the number of vectors to be orthonormalized, another manner, [JAM 02], to built up a new basis (W_i) from the vectors U_i is proposed with the following procedure:

$$\left\{ \begin{array}{l} \text{for } i = 1, \dots, l \\ W_i = U_i \\ \\ \text{for } i = l + 1, \dots, p \\ W_i = U_i - \sum_{k=1}^{i-1} \alpha_k^i W_k \\ \langle W_i, U_j \rangle = 0 \text{ for } j = 1, \dots, i - 1 \end{array} \right. \quad [19]$$

where l is an integer ($1 \leq l \leq p$) from which the two bases differ and α_k^i are scalar coefficients. In [19], only the $p - l$ last vectors are orthonormalized. We can rewrite this new basis (W_i) as $(U_1, \dots, U_l, W_{l+1}, W_{l+2}, \dots, W_p)$. With the procedure [19], the vectors W_i ($l + 1 \leq i \leq p$) are orthogonal to the vectors (U_j) ($1 \leq j \leq i - 1$).

From [19], we obtain for $i = l + 1, \dots, p$:

$$\begin{cases} \text{for } j = 1, \dots, i - 1 \\ \langle U_i, U_j \rangle = \sum_{k=1}^l \alpha_k^i \langle U_k, U_j \rangle + \sum_{k=l+1}^{i-1} \alpha_k^i \langle W_k, U_j \rangle \end{cases} \quad [20]$$

At each order $i \geq l+1$, the coefficients α_k^i are solutions of the following linear system:

$$\begin{bmatrix} \langle U_1, W_1 \rangle & \dots & \langle U_1, W_{i-1} \rangle \\ \vdots & \vdots & \vdots \\ \langle U_{i-1}, W_1 \rangle & \dots & \langle U_{i-1}, W_{i-1} \rangle \end{bmatrix} \begin{bmatrix} \alpha_1^i \\ \vdots \\ \alpha_{i-1}^i \end{bmatrix} = \begin{bmatrix} \langle U_1, U_i \rangle \\ \vdots \\ \langle U_{i-1}, U_i \rangle \end{bmatrix} \quad [21]$$

Let us remark that the resolution of this linear system [21], necessitates only the knowledge of the vectors W_i at previous orders $k \leq i - 1$. Particularly at the order $i = l + 1$, the matrix of the linear system [21] depends only on the vectors $(U_k)_{k=1}^l$. So we can compute the coefficients α_k^i and the vectors W_i recurrently from the order $i = l + 1$. If we introduce the notations

$$\begin{aligned} & \text{for } i = 1, \dots, l : \\ & \alpha_k^i = \begin{cases} 0 & \text{if } k = 1, \dots, i - 1 \\ 1 & \text{if } k = i \end{cases} \end{aligned} \quad [22]$$

$$\begin{aligned} & \text{for } i = l + 1, \dots, p : \\ & \alpha_i^i = 1, \end{aligned}$$

the vectors $(U_i)_{i=1}^p$ can be written in the new basis $(W_i)_{i=1}^p$ as follows:

$$U_i = \sum_{k=1}^i \alpha_k^i W_k \quad [23]$$

and the polynomial representation [2] can be written in the new basis under the form:

$$\begin{aligned} U_{pol(p)}(a) &= U_0 + ag^1(a)W_1 + a^2g^2(a)W_2 + \dots + a^p g^p(a)W_p \\ &= U_0 + \sum_{i=1}^l a^i g^i(a)U_i + \sum_{i=l+1}^p a^i g^i(a)W_i \end{aligned} \quad [24]$$

where the component functions g^i are scalar series defined by:

$$g^i(a) = \sum_{k=0}^{p-i} \alpha_i^{k+i} a^k \quad [25]$$

The representation [24] may be truncated at an order q . To obtain rational representations, one replaces the scalar series g^i by Padé approximants with a common denominator $g^i[L^i, M] = \frac{A^i}{B}$. The polynomials A^i and B are respectively of degrees L^i and M and satisfy ($K^i = L^i + M$):

$$Bg^i(a) - A^i(a) = O(a^{K^i+1}) \quad [26]$$

From the relation [26], a linear system permits to compute the coefficients A_k^i and B_k .

$$\begin{cases} \text{for } i = 1, \dots, q : \\ \left\{ \begin{array}{ll} \sum_{k=0}^j B_k g_{j-k}^i - A_j^i = 0 & \text{for } j = 0, \dots, L^i \\ \sum_{k=0}^j B_k g_{j-k}^i = 0 & \text{for } j = L^i + 1, \dots, K^i \end{array} \right. \end{cases} \quad [27]$$

Let us notice that we must have $M = \sum_{i=1}^q (K^i - L^i)$ to obtain a linear system with the same number of rows and columns. The parameter λ is also approximated by a rational fraction $\frac{A^\lambda}{B}$ where A^λ is a polynomial of degree L^λ satisfying:

$$B\lambda(a) - A^\lambda(a) = O(a^{L^\lambda+1}) \quad [28]$$

So a new family of vectorial Padé approximants is obtained:

$$\begin{aligned} U_{rat(p)}(a) &= U_0 + \sum_{i=1}^q a^i g^i[L^i, M](a) W_i \\ \lambda_{rat(p)}(a) &= \lambda[L^\lambda, M](a) \end{aligned} \quad [29]$$

The rational representation [29] is defined by the choice of the number l , which defines the range from which we construct the new basis, by the order of truncature q and by the degrees $(K^i)_{i=1}^q$, $(L^i)_{i=1}^q$ and L^λ .

2.4. Continuation procedure

The representations [2], [16] or [13], [17] or [18] or [29] permit to compute only a part of the solution path. To obtain the entire solution path, Cochelin [COC 94c] proposed a continuation procedure for the vectorial series representation [2] based on the following criterion:

$$a_{maxs} = (\epsilon_{pol} \frac{\|U_1\|}{\|U_p\|})^{\frac{1}{p-1}} \quad [30]$$

which gives an evaluation of the domain of validity of the polynomial representation. Once the determination of the domain of validity is done, by the computation of the radius of validity a_{maxs} for a fixed tolerance ϵ_{pol} , the vectorial series representation [2] can be applied in a continuation procedure to obtain the entire solution path step by step.

To introduce the vectorial Padé representation [13], [17] in a continuation algorithm, Elhage et al. [ELH 00] proposed another criterion defined by:

$$\frac{\|U_{pad(p)}(a_{maxp}) - U_{pad(p-1)}(a_{maxp})\|}{\|U_{pad(p)}(a_{maxp}) - U_0\|} = \epsilon_{pad} \quad [31]$$

which gives an evaluation of the radius of validity a_{maxp} of the rational representation [13], [17] for a fixed tolerance ϵ_{pad} , by using a dichotomy process.

We shall use the same criterion [31] to introduce the two proposed vectorial Padé representations [18] and [29] in a continuation process.

3. Numerical results and discussion

3.1. Definition of the tests and of the Padé approximants

The numerical robustness of the approximations obtained by the vectorial series representation and by the different vectorial Padé representations is discussed on the basis of tests emanating from non-linear elastic thin shell analysis.

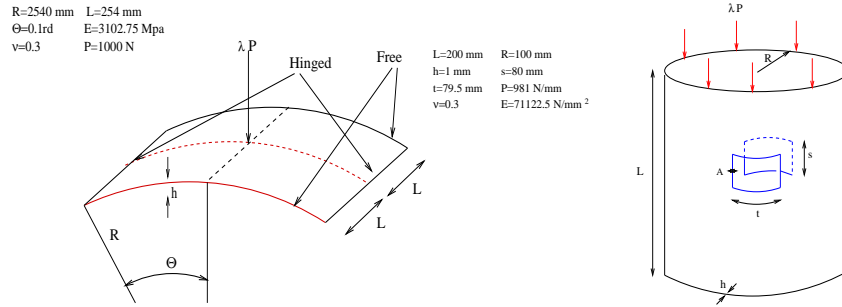


Figure 1. (a) Cylindrical roof loaded in its center, (b) Cut out cylinder with a compression load

The first example is a cylindrical roof hinged along two opposite sides and submitted to a concentrated force λP at the central point (figure 1-a). By assuming symmetry conditions, only one quarter of the shell is discretized with 200 triangular *DKT18* elements for a total number of degrees of freedom equal to 726. The analysis is carried out with two different values of the thickness: $h_1 = 12.7$ mm and $h_2 = 6.35$ mm.

The second example is a cylinder with two diametrically opposite cut out loaded by a uniform compression λP (figure 1-b). For symmetry reasons, one eighth of the structure is discretized with 1608 triangular *DKT18* elements. The total number of degrees of freedom is 5190.

On these figures, the approximations are labelled:

- *pol* if we use the vectorial series representation [2], [16],
- *pad* if we use the usual vectorial Padé representation [13], [17],
- *npad* if we use the improved vectorial Padé representation [18]
- *rat* if we use the new representation [29] and if the series [24] is truncated at the order $q = p - 1$
- *nrat* if we use [29] and if the series [24] is truncated at the order $q = p$.

The quality of one ANM step is evaluated from load-deflection curves and residual-deflection curves and the main criterion is the step length. These curves are reported on figures 2, 3, 4, 5, 6.

For the orthonormalization of the basis, the modified Gram-Schmidt algorithm, presented in the fourth part, has been used.

To analyse the quality of the new rational representation [29], we shall test different values of the number l (l is the number of vectors that are not orthonormalized) and two sorts of choices for the degrees K^i , L^i , L^λ according to the order of truncature q of the series [24]:

$$\left\{ \begin{array}{l} q = p - 1 \\ K^i = p - i \quad i = 1, \dots, q \\ L^i = p - i - 1 \quad i = 1, \dots, q \\ L^\lambda = p - 1 \end{array} \right. \quad [32]$$

$$\left\{ \begin{array}{l} q = p \\ K^i = p - i \quad i = 1, \dots, q \\ L^i = p - i - 1 \quad i = 1, \dots, p - 1, L^p = 0 \\ L^\lambda = p \end{array} \right. \quad [33]$$

The approximations corresponding to the choices $l = p - 5$, $p - 4$, $p - 2$ and $p - 1$ are respectively labelled *rat1*, *rat2*, *rat3* and *rat4* for the degrees in [32] and respectively labelled *nrat1*, *nrat2*, *nrat3* and *nrat4* for the degrees in [33].

3.2. Single step analysis

We compare the different vectorial Padé approximations in the case of the cylindrical roof ($h_1 = 12.7$) at order $p = 6$ on the figure 2 and at order $p = 20$ on the figure 6. For the cut out cylinder, the approximations at order $p = 8$ are compared on the figure 3. For the cylindrical roof with $h_2 = 6.35$, the approximations at order $p = 12$ are compared on the figure 4 and the approximations at order $p = 18$ are compared on the figure 5. The reference curves (labelled *ref*) have been obtained by the Newton-Raphson method.

If the range of validity (r.o.v) of each approximation is defined by assigning a maximal value of the norm of the residual vector, the r.o.v of the polynomial representation (*pol*), except for the case at order $p = 6$, is lower than the one of all vectorial Padé

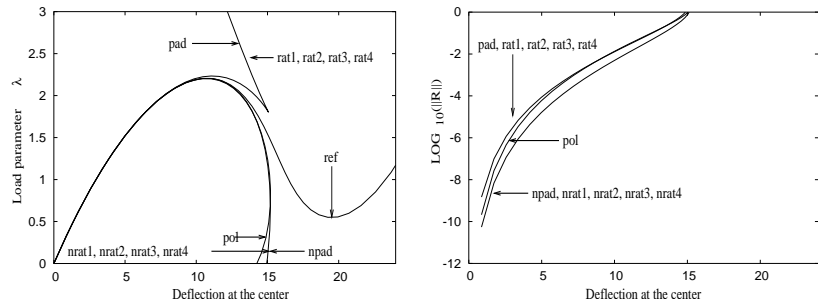


Figure 2. (a) Load-displacement and (b) residual curves for the cylindrical roof: $h_1 = 12.7$, order $p = 6$

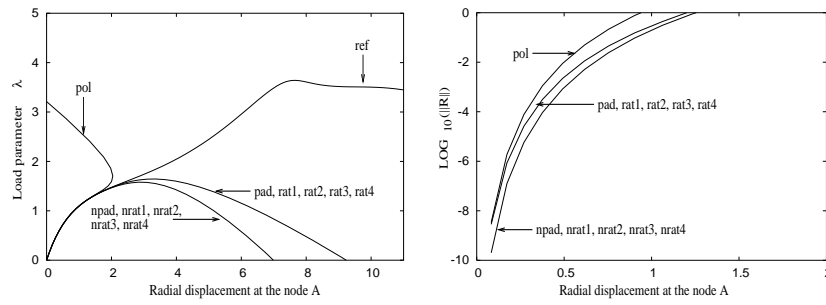


Figure 3. (a) Load-displacement and (b) residual curves for the cut out cylinder: Order $p = 8$

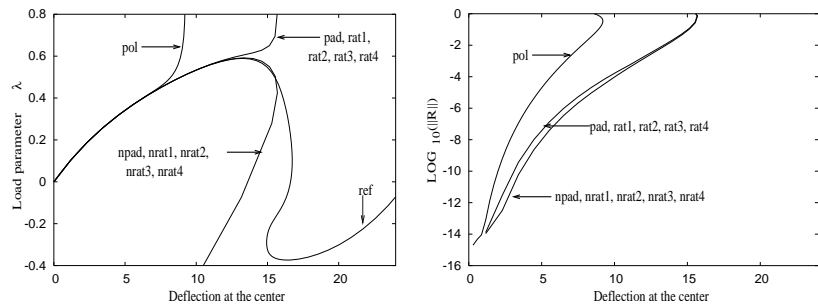


Figure 4. (a) Load-displacement and (b) residual curves for the cylindrical roof: $h_2 = 6.35$, order $p = 12$

approximations. For all these approximations a large order of truncature increases the r.o.v.

The largest r.o.v is always obtained by the use of the new vectorial Padé approximant ($npad, nrat$) i.e. when we keep the last term in the series [12].

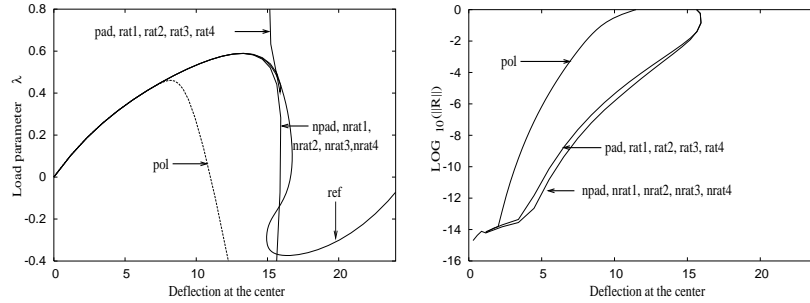


Figure 5. (a) Load-displacement and (b) residual curves for the cylindrical roof: $h_2 = 6.35$, order $p = 18$

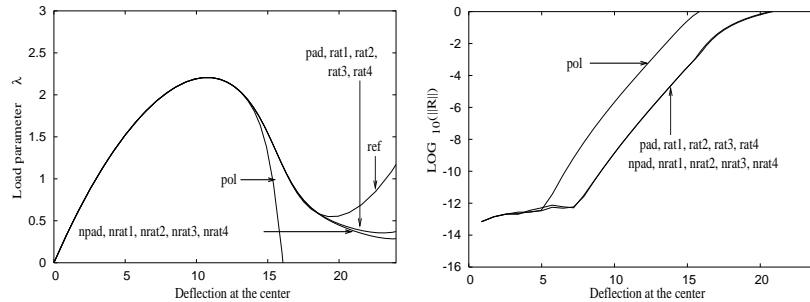


Figure 6. (a) Load-displacement and (b) residual curves for the cylindrical roof: $h_1 = 12.7$, order $p = 20$

One can observe from figure 2 that for small orders ($p = 6$), the r.o.v of the polynomial representation (pol) is larger than the one of the vectorial Padé approximants (pad, rat), i.e. no convergence acceleration, while the r.o.v of the new vectorial Padé approximants ($npad, nrat$) seems larger. Thus for a small order of truncature it is interesting to keep the last term in the series [12] to define Padé approximants.

In the case of the vectorial Padé approximants ($rat, nrat$) [29], one can see from the figures (2, 3, 4, 5, 6) that, for each example and for each order, there is no influence of the parameter l (the number of vectors that are not orthonormalized). Indeed these figures show that the curves $rat1, 2, 3, 4$ (respectively $nrat1, 2, 3, 4$) coincide for each example and for each order. For instance, in the case of an order of truncature

$p = 20$, the curve *rat1* in the figure 6 has been obtained by orthonormalizing only the last 5 vectors. Hence it seems very interesting to use this representation in order to avoid a large number of vectors orthonormalization.

3.3. Multi-step analysis

We consider now two numerical examples in order to discuss the continuation algorithm based on vectorial Padé approximations. In this comparison, the total number of steps is the measure of the efficiency of the algorithms.

In the many numerical experimentations that have been done [JAM 02], the continuation algorithm based on vectorial Padé approximants is more attractive than the one based on the vectorial series representation. The use of vectorial Padé approximations decreases considerably the number of steps.

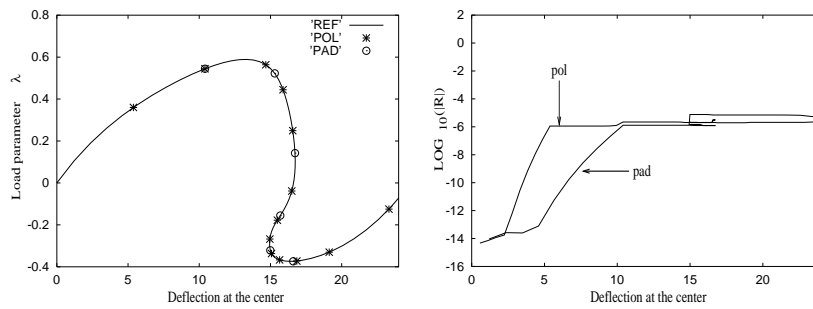


Figure 7. (a) Load-displacement and (b) residual curves for the cylindrical roof: $h_2 = 6.35$, order $p = 20$, $\epsilon_{pol} = \epsilon_{pad} = 10^{-8}$

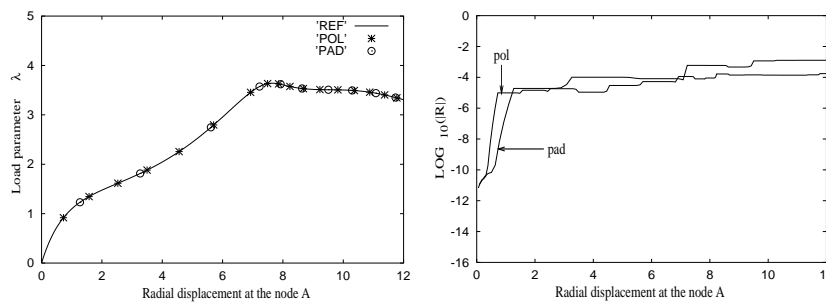


Figure 8. (a) Load-displacement and (b) residual curves for the cut out cylinder: Order $p = 20$, $\epsilon_{pol} = 10^{-8} = \epsilon_{pad}$

For the following tests, the accuracy parameters, in criterion [30], [31], are chosen as $\epsilon_{pol} = \epsilon_{pad} = 10^{-8}$ and we consider the truncation order $p = 20$.

In the case of the cylindrical roof with a thickness $h_2 = 6.35$, figure 7, the number of steps to get the solution until a deflection $w = 16.85$ is reduced from 11 with the series (*pol*) to 6 with the classical vectorial Padé approximants (*pad*). Thus the number of steps is reduced by a factor of two.

For the cut out cylinder, figure 8, the number of steps to get the solution until a radial displacement $r = 11.8$ is reduced from 17 with the series (*pol*) to 10 with the classical vectorial Padé approximants (*pad*).

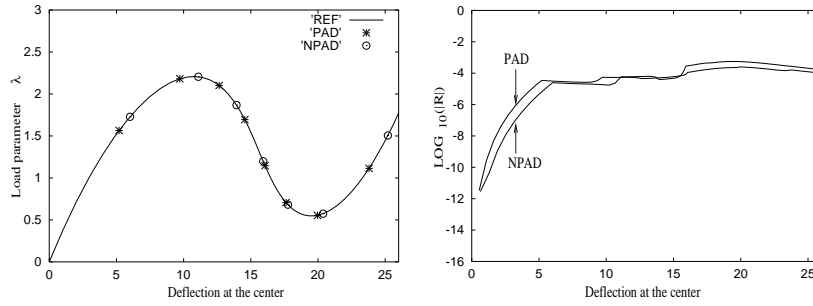


Figure 9. Load-displacement and residual curves for the cylindrical roof with $h_1 = 12.7$: Order $p = 8$, $\epsilon_{pol} = 10^{-6}$, $\epsilon_{pad} = 10^{-6}$, $\epsilon_{npad} = 10^{-5}$. Comparison of two Padé approximants in a continuation process.

For the chosen accuracy parameters, the residual remains almost constant along the solution path except for the first step, see figure 7-b for the cylindrical roof and figure 8-b for the cut out cylinder. The residual remains small along the solution path: it is lower than 10^{-6} for the cylindrical roof and it is lower than 10^{-4} for the cut out cylinder. So the continuation algorithm provides a satisfactory solution without any corrections for the chosen accuracy parameters.

We consider now two numerical examples in order to discuss the continuation algorithm based on the usual vectorial Padé representation *pad* [13], [17], and the improved vectorial Padé representation *npad* [18] with a small truncation order.

For the first test: cylindrical roof with a thickness $h_2 = 12.7$ (see figure 9), the accuracy parameters are chosen as $\epsilon_{pol} = \epsilon_{pad} = 10^{-6}$, $\epsilon_{npad} = 10^{-5}$ and we consider the truncation order $p = 8$. These values of ϵ_{pad} and ϵ_{npad} have been chosen to yield about the same residual curve.

The number of steps to get the solution until $w = 24$ is equal to 8 with the usual vectorial Padé representation *pad* and only equal to 7 to get the solution until $w = 25$ with the improved vectorial Padé approximants (*npad*), see figure 9-a. From figure

9-b, one checks that, for the chosen accuracy parameters, the residual remains small and the same for the two approximations.

For the second test: cylindrical roof with a thickness $h_2 = 6.35$ (see figure 10), the accuracy parameters, in criterion [30], [31], are chosen as $\epsilon_{pol} = 10^{-7}$, $\epsilon_{pad} = 4.10^{-7}$, $\epsilon_{npad} = 2.10^{-7}$ and we consider the truncation order $p = 12$. In this test 13 steps permit to obtain the solution until $w = 21$ with the usual vectorial Padé representation pad and until $w = 25$ with the improved vectorial Padé approximants $npad$ (see figure 10-a). The residual (figure 10-b) remains small and the same for the two approximations.

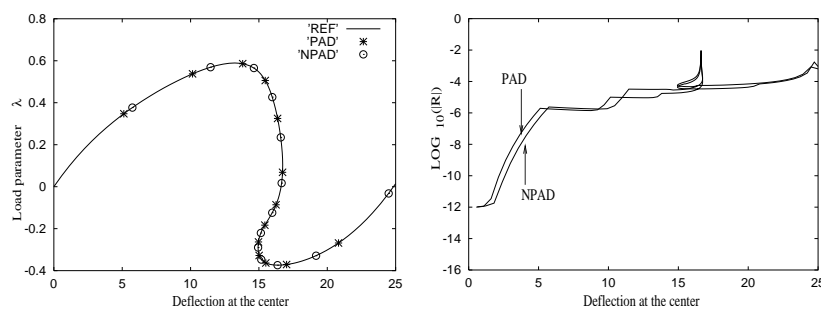


Figure 10. Load-displacement and residual curves for the cylindrical roof with $h_2 = 6.35$: Order $p = 12$, $\epsilon_{pol} = 10^{-7}$, $\epsilon_{pad} = 4.10^{-7}$, $\epsilon_{npad} = 2.10^{-7}$

4. Influence of the Gram-Schmidt orthonormalization and the scalar product

4.1. Gram-Schmidt orthonormalization procedures

Let us recall that a process of orthonormalization is a numerical instability source [LIN 00]. There are numerical instabilities in the computation of the Gram-Schmidt coefficients $\alpha_{i,j}$ and the latter can change all the coefficients B_i . So we must be able to compute accurately the coefficients $\alpha_{i,j}$. This point has been discussed in [NAJ 96], [CHA 97], [NAJ 98], [JAM 02], in the case of an elastic beam subjected to a bending force. The comparison between the exact coefficients of Gram-Schmidt procedure using a symbolic software (MAPLE) and those obtained by finite elements shows that numerical errors are accumulated and that the new vectors U_i^* are completely false beyond a certain order.

Results in [CHA 97] clearly show the influence of the orthonormalization without establishing if instabilities are due to the orthonormalization or something else as the calculation of the vectors themselves. One can also note that these instabilities do not prevent a better solution quality than the series nor a good evaluation of the smallest pole, that is assimilated to the radius of convergence [ELH 00]. But one has

also observed, especially in iterative algorithms, that the residual-order curves had a bizarre behaviour at large orders, that let suppose a harmful numerical instability effect [MAL 99], [MAL 00]. Is one able to reduce them while only changing the technique of orthonormalization or the scalar product?

The classical Gram-Schmidt algorithm (CGS) is summarized in the first column of the table 1. We have observed in many tests that, using this algorithm, the new vectors U_i^* are completely false beyond a small order [NAJ 96], [NAJ 98]. It is known that the modified Gram-Schmidt algorithm (MGS), which is summarized in the second column of the table 1, provides a better stability.

The accuracy of the classical Gram-Schmidt algorithm can be vastly improved by applying it iteratively. This so-called iterated Gram-Schmidt procedure has been used in [HOF 89]. This algorithm (IGS), which is an iterative version of the classical one, is presented in the third column of the table 1. Let us notice that with one iteration of IGS, for each vector, we get back the CGS algorithm. An important part of the algorithm is the stopping criterion $\|U_i^{*k}\| > \beta \|U_i^{*(k-1)}\|$ which depends on an arbitrary parameter β . In [HOF 89], [JAM 02], it has been shown that the IGS algorithm converges within two iterations with $\beta \approx 0.5$.

CGS	MGS	IGS
<pre> for i=1, ..., p do for j=1, ..., i-1 $\alpha_{i,j} = \langle U_i, U_j^* \rangle$ enddo $q_i = U_i - \sum_{j=1}^{i-1} \alpha_{i,j} U_j^*$ $U_i^* = q_i / \ q_i\$ enddo </pre>	<pre> for i = 1, ..., p do $q_i = U_i$ for j=1, ..., i-1 $\alpha_{i,j} = \langle q_i, U_j^* \rangle$ $q_i = q_i - \alpha_{i,j} U_j^*$ enddo $U_i^* = q_i / \ q_i\$ enddo </pre>	<pre> for i = 1, ..., p do $U_i^{*0} = U_i, \alpha_{i,j}^0 = 0$ for k = 1, 2, ... do for j = 1, ..., i - 1 do $\gamma_{i,j}^k = \langle U_i^{*(k-1)}, U_j^* \rangle$ $\alpha_{i,j}^k = \alpha_{i,j}^{k-1} + \gamma_{i,j}^k$ enddo $U_i^{*k} = U_i^{*(k-1)} - \sum_{j=1}^{i-1} \gamma_{i,j}^k U_j^*$ if ($\ U_i^{*k}\ > \beta \ U_i^{*(k-1)}\$) then stop endif enddo $U_i^* = U_i^{*k} / \ U_i^{*k}\$ for j = 1, ..., i - 1 do $\alpha_{i,j} = \alpha_{i,j}^k$ senddo enddo </pre>

Table 1. The classical (CGS), modified (MGS) and iterated (IGS) Gram-Schmidt algorithms

4.2. Comparison of the three Gram-Schmidt orthonormalizations

In this section, we choose $\beta = 0.5$ for the iterated Gram-Schmidt (IGS) algorithm. To analyse the quality of the Gram-Schmidt algorithms (CGS, MGS and IGS), we consider the criterion e_p defined by:

$$e_p = \|Q_p^T Q_p - I_p\| \quad [34]$$

where the matrix Q_p is $(U_1^*, \dots, U_{p-1}^*)$, I_p is the identity matrix. In this section the scalar product used, for the three Gram-Schmidt algorithms, is the ordinary scalar product defined by $\langle U, V \rangle_{ORD} = \sum_{k=1}^N U_k V_k$ where $U = (U_k)_{k=1}^N$ and $V = (V_k)_{k=1}^N$.

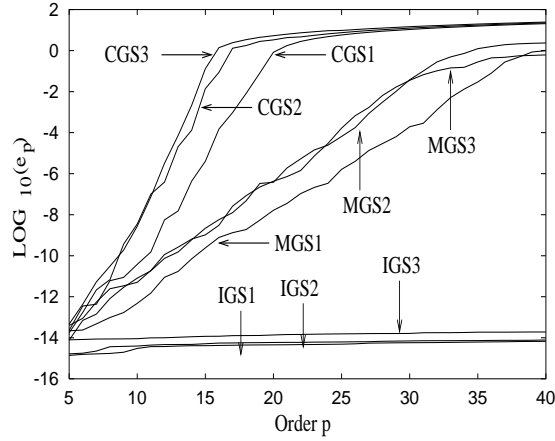


Figure 11. Precision e_p versus the order p

Let us recall that theoretically $(\langle U_i^*, U_j^* \rangle)_{1 \leq i, j \leq p} = I_p$. Therefore, the precision e_p analyses the quality of the orthonormalization of the basis (U_i^*) .

In figure 11, we represent the decimal logarithm of the precision e_p versus the order of truncature p . The curves (CGS1, MGS1, IGS1) and (CGS2, MGS2, IGS2) correspond to the cylindrical roof respectively with the thickness $h_1 = 12.7$ and $h_2 = 6.35$ and (CGS3, MGS3, IGS3) correspond to the cut out cylinder [JAM 02], [JAM 03].

We observe in these tests (figure 11) that the better accuracy is obtained using the IGS algorithm and that the CGS algorithm is the least accurate. The behavior of the criterion [34] shows that the algorithm IGS is stable until the order $p=40$ while the CGS and MGS algorithms loose their precision at respectively the orders $p \simeq 15$ and $p \simeq 30$.

4.3. Influence of the scalar product

Let us notice that the vectors and the coefficients generated by Gram-Schmidt procedure depend on the choice of the scalar product.

In this section we analyse the influence of the scalar product on the residual curve of the classical rational representation at order 30 and order 60 in the case of the cylindrical roof ($h_2 = 12.7$). We use for this analysis two sorts of scalar product: the ordinary scalar product (noted $\langle \cdot, \cdot \rangle_{ORD}$) and the mass scalar product defined by $\langle U, V \rangle_{MAS} = U^T M V$ where M is the mass matrix.

The figure 12 give the influence of the choice of the scalar product (ORD for ordinary scalar product and MAS for mass scalar product) and the choice of the orthonormalization algorithm (CGS, MGS, IGS) on the classical vectorial representation of one ANM step at orders 30 and 60.

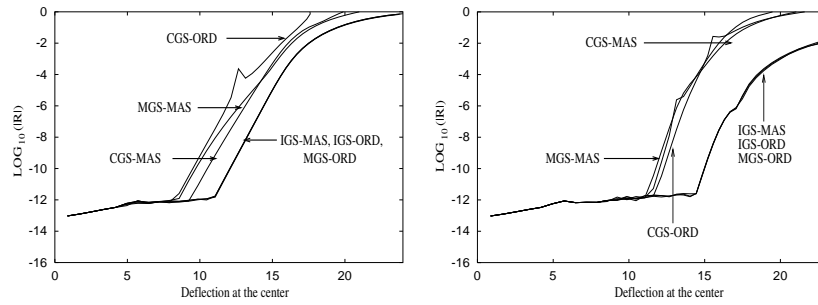


Figure 12. Residual curves for the cylindrical roof with $h_1 = 12.7$: (a) order $p = 30$, (b) order $p = 60$

One can see from this figure that if the IGS algorithm is used, the same result is obtained for the two scalar products. The same behaviour is obtained when we use the CGS algorithm. Hence there is no influence of the scalar product on these two orthonormalization algorithms IGS and CGS. Let us notice that the accuracy of the solution with IGS is better than the one with CGS. These results are not surprising because the algorithm IGS is an iterative version of the classical one CGS.

The figure 12 shows clearly that, when we use the MGS algorithm (usually used in the ANM), the residual curves change with the choice of the scalar product. Indeed when we choose the ordinary scalar product, the residual curves obtained by using the MGS algorithm coincide with those obtained by using the IGS algorithms and when we choose the mass scalar product, the residual curves obtained by the MGS algorithm coincide with those obtained by the CGS algorithm.

The Gram-Schmidt algorithms have been tested in the ANM continuation with a large truncation order $p = 28$, by using the ordinary scalar product (figure 13-a) and the mass scalar product (figure 13-b).

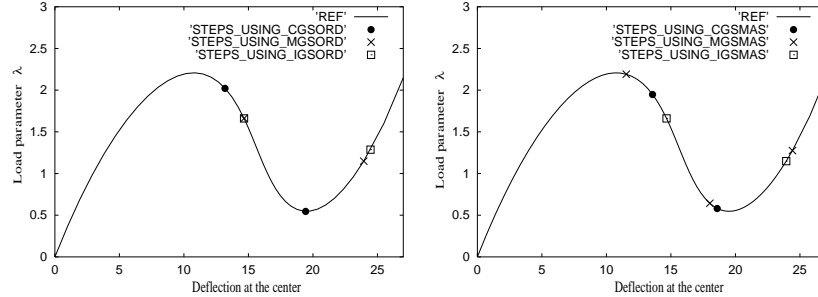


Figure 13. Load-displacement curves for the cylindrical roof with $h_1 = 12.7$ at the order $p = 28$

One can see from the figure 13-a that if we use the ordinary scalar product, two ANM steps coupled with IGS are slightly better than two ANM steps coupled with MGS.

And from the figure 13-b, one can see that if we use the mass scalar product, two ANM steps coupled with IGS are slightly equivalent to three ANM steps coupled with MGS.

Thus for large order it seems more interesting to use IGS algorithm for orthonormalizing the basis.

5. Quadratic representation

The second and the third parts show us that one can improve clearly the domain of validity of the polynomial representation by using Padé approximants. Can the domain of validity of the rational representation be still improved by using another approximants?

To define quadratic approximants [SHA 74] in the Asymptotic Numerical Method, one can apply the same technique of orthonormalization, previously considered in the section 2 for Padé approximants, and replace the components functions f^i by quadratic approximants $f^i[L^i, M^i, N^i]$. This work has been published in [JAM 01] and an example of plate shows that good approximations are obtained with the quadratic representation but with a lot of poles in the domain of validity.

To avoid the apparition of poles, we consider quadratic approximants having two polynomials in common. The idea, [JAM 01], [JAM 02], is to replace the series f^i by quadratic approximants $f^i[L^i, M, N] = \frac{-B \pm \sqrt{B^2 - A^i C}}{C}$ having the two polynomials B and C in common and solutions of the quadratic equations:

$$C f^i[L^i, M, N]^2 + 2B f^i[L^i, M, N] + A^i = 0 \quad [35]$$

The polynomials (A^i) , B and C have respectively for degrees (L^i) , M and N and satisfy the relation:

$$C(f^i)^2 + 2Bf^i + A^i = O(a^{K^i+1}) \quad [36]$$

where (K^i) are arbitrary integers. To compute the coefficients of polynomials (A^i) , B and C , linear equations are deduced by identification:

for $i = 1, \dots, q$

$$\left\{ \begin{array}{l} \text{for } j = 0, \dots, L^i \\ \sum_{k=0}^j C_k \delta_{j-k}^i + 2 \sum_{k=0}^j B_k f_{j-k}^i + A_j = 0 \end{array} \right. \quad [37]$$

$$\left\{ \begin{array}{l} \text{for } j = L^i + 1, \dots, K^i \\ \sum_{k=0}^j C_k \delta_{j-k}^i + 2 \sum_{k=0}^j B_k f_{j-k}^i = 0 \end{array} \right. \quad [38]$$

where the coefficients f_k^i and δ_k^i are respectively the coefficients of the series f^i and $(f^i)^2$:

$$\begin{aligned} f^i(a) &= \sum_{k=0}^{p-i} f_k^i a^k = \sum_{k=0}^{p-i} \alpha_{i,k+i}^i a^k, \\ (f^i)^2(a) &= \sum_{k=0}^{p-i} \delta_k^i a^k \text{ with } \delta_j^i = \sum_{k=0}^j f_k^i f_{j-k}^i \end{aligned}$$

The degrees K^i are chosen such that $\sum_{i=1}^q (K^i - L^i) = M + N + 1$. The linear equations [38] permit to construct a linear system which defines the coefficients (B_k) and (C_k) with a normalization condition on one coefficient of the polynomials B or C , for instance $C_0 = 1$. So the coefficients A_k^i can be computed from relations [37].

For the quadratic approximation of the load parameter λ , the parameter $\lambda^*(a) = \frac{\lambda(a) - \lambda_0}{a}$ is replaced by a quadratic approximant $\lambda^*[L^{\lambda^*}, M, N]$ having the same polynomials B and C . So only the coefficients of the polynomial A^{λ^*} have to be computed by the relation:

$$\left\{ \begin{array}{l} \text{For } j = 0, \dots, L^{\lambda^*} \\ A_j^{\lambda^*} = \sum_{k=0}^j C_k \delta_{j-k}^{\lambda^*} + 2 \sum_{k=0}^j B_k \lambda_{j-k}^{\lambda^*} \end{array} \right. \quad [39]$$

After having computed all the coefficients of polynomials (A^i) , A^{λ^*} , B and C , the sign \pm has to be chosen in the quadratic approximation. The algorithm proposed in the table 2 is a method to choose the sign \pm . The aim of this algorithm is to obtain the solution which has the best Mac-Laurin development.

Then the vectorial quadratic representation of the solution is defined by:

$$\left\{ \begin{array}{l} [U_{quad(p)}(a)] = [U_0] + \sum_{i=1}^q a^i f^i [L^i, M, N](a) [U_i^*] \\ \lambda_{quad(p)}(a) = \lambda_0 + a \lambda^* [L^{\lambda^*}, M, N](a) \end{array} \right. \quad [40]$$

On figure 14, the quadratic representation [40] (labelled *apq*) has been compared to the polynomial representation (labelled *pol*) and to the classical rational representation (labelled *pad*) by considering the following choice of degrees :

$$\begin{cases} q = p \\ K^i = p - i \text{ for } i = 1, \dots, q \\ L^i = p - i - 2 \text{ for } i = 1, \dots, 14 \\ L^i = p - i \text{ for } i = 15, \dots, p \\ M = 29 - p, N = p - 2 \\ L^{\lambda^*} = p - 1 \end{cases} \quad [41]$$

We note on the load-displacement curves (figure 14), that the prediction of the solution by the quadratic representation *apq* is better than the polynomial representation *pol*. But the better prediction seems to be the rational representation *pad* for this choice and this example.

<p>1• Compute the polynomial development of $\sqrt{W^i}$ ($W^i = B^2 - A^i C$)</p> <p style="text-align: center;">↓</p> <p>2• If there is $\beta = \pm 1$ such that $Cf^i + B + \beta\sqrt{W^i} = 0$ then choose the sign of $-\beta$</p> <p style="text-align: center;">↓</p> <p>3• Else compute the numbers d_{+1} and d_{-1} from the relation</p> $Cf + B \pm \sqrt{W} = O(a^{d_{\pm 1}})$ <ul style="list-style-type: none"> • If $d_{+1} \leq d_{-1}$, choose the sign +. • Else choose the sign -.

Table 2. Algorithm of the choice of the sign \pm for quadratic approximants

In [JAM 02], a lot of choice of quadratic approximations has been considered for all the tests presented in this paper but we have not found yet a good strategy, except for the example of a plate loaded in its center (figure 15). For this example we have done the following choice (labelled *apq*).

$$\begin{cases} q = p \\ K^i = p - i \text{ for } i = 1, \dots, q \\ L^i = p - i - 6 \text{ for } i = 1, \dots, L_M = E(\frac{2p-1}{6}) \\ L^i = p - i \text{ for } i = L_M + 1, \dots, p \\ M = p - 1, N = L_M * 6 - p \\ L^{\lambda^*} = p - 1 \end{cases} \quad [42]$$

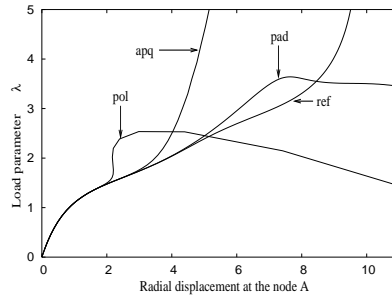


Figure 14. (a) Load-displacement and (b) residual curves for the cut out cylinder at the order $p = 20$

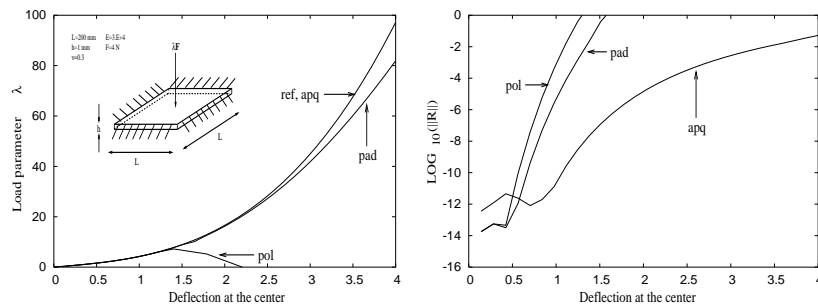


Figure 15. Load-displacement curves for the plate problem at the order $p = 28$

repr.	pol	pad	apq
Step 1	$w = 1.0269$	$w = 1.2522$	$w = 3.06571$
Step 2	$w = 2.1089$	$w = 2.7581$	$w = 13.7847$

Table 3. Deflection w for each step of continuation for the plate problem: Order $p=26$

The results for this choice are plotted on figure 15. The figure 15-a shows that a spectacular improvement is obtained with the quadratic representation. The reference curve is recovered up to a deflection 4 whereas the polynomial and rational representations coincide with the reference curve until a deflection respectively of about 1.4 and 2. On the figure 15-b, the quadratic representation shows a better precision than the representations *pol* and *pad*. For a maximal precision of 10^{-4} , we get a deflection of about 2.3 by using the quadratic representation (*apq*) and only a deflection of about 1.2 and 0.9 by using respectively the rational (*pad*) and the polynomial (*pol*) representations.

For the same example, the choice [42] has been considered in ANM continuation process. The results are presented in table 3. This table show clearly that the rational representation is improved by quadratic approximants. If we use the vectorial quadratic representation, one multiplies by three the range of validity obtained by the polynomial representation and by two the range of validity obtained by the classical rational representation. Two steps with the quadratic representation, multiply by 5 the range of validity obtained by two steps with the rational representation.

6. Conclusion

In this paper, 3 sorts of vectorial Padé approximants have been defined to increase the range of validity of the vectorial series approximation in the Asymptotic Numerical Method.

The numerical experimentation, on non-linear shell problems, has shown that these vectorial Padé approximants extend the range of validity and reduce the number of steps needed in the ANM path following technique. From these tests, one can conclude that, first, it is interesting to keep the last term in the series [12] particularly for small order of truncature (the improved vectorial Padé representation [18]). Second, it seems very interesting to use the new vectorial Padé representation [29] in order to avoid a large number of vectors orthonormalization.

We also showed that the better results, especially for large orders, are always obtained by the iterative version of the classical Gram-Schmidt algorithm (IGS) and, moreover, the efficiency of the IGS algorithm does not depend on the scalar product.

In the last section, we have defined vectorial quadratic approximants in the ANM. In a specific case, these approximants have been proved very effecient.

7. References

- [AZR 92] AZRAR L., COCHELIN B., DAMIL N., POTIER-FERRY., *An asymptotic-numerical method to compute bifurcating branches*, In: Ladevèze, P., Zienkiewicz, O.C. (Eds), *New Advances in Computational Structural Mechanics*. Elsevier, Amstredam, p. 117–131, 1992.
- [BAK 96] BAKER G. A. JR., GRAVES MORRIS P., *Padé approximants*, *Encyclopedia of Mathematics and its application*, VOL. 59, 2ND EDITION, 1996.
- [BRA 95] BRAIKAT B., *Méthode asymptotique numérique et fortes non linéarités*, *Thèse de 3ème cycle, Université Hassan II - Mohammedia, Faculté des Sciences Ben M'Sik, Casablanca, Maroc*, 1995.
- [BRA 97] BRAIKAT B., DAMIL N., POTIER-FERRY., *Méthodes asymptotiques numériques pour la plasticité*, *Revue Européenne des Eléments Finis*, VOL. 6, p. 337–357, 1997.
- [BRE 94] BREZINSKI C., ISEGHEM V., *Padé approximants*, In: Ciarlet, P.G., Lions, J.L. (Eds), *Handbook of Numerical Analysis*, VOL. 3, NORTH-HOLLAND, AMSTERDAM, 1994.

- [CAD 01] CADOU J.M., MOUSTAGHIFIR N., MALLIL E., DAMIL N., POTIER-FERRY., *Linear iterative solvers based on perturbation method*, *Comptes Rendus de l'Académie des Sciences, Paris*, VOL. 329, SÉRIE II B, P. 457–462, 2001.
- [CHA 97] CHARI R., *Analyse non linéaire des structures en treillis par la M.E.F. et influence de la procédure d'orthogonalisation et du produit scalaire sur les approximants de Padé*, *Thèse de 3ème cycle, Université Hassan II - Mohammedia, Faculté des Sciences Ben M'Sik, Casablanca, Maroc*, 1997.
- [COC 94A] COCHELIN B., DAMIL N., POTIER-FERRY., *Asymptotic-numerical methods and Padé approximants for non-linear elastic structures*, *International Journal for Numerical Method in Engineering*, VOL. 37, P. 1187–1213, 1994.
- [COC 94B] COCHELIN B., DAMIL N., POTIER-FERRY M., *The asymptotic-numerical method: an efficient perturbation technique for non linear structural mechanics*, *Revue Européenne des Eléments Finis*, VOL. 3 (2), P. 281–297, 1994.
- [COC 94C] COCHELIN B., *A path following technique via an asymptotic numerical method*, *Computers and Structures*, VOL. 53, P. 1181–1192, 1994.
- [DAM 90] DAMIL N., POTIER-FERRY., *A new method to compute perturbed bifurcation, Application to the buckling of imperfect elastic structures*, *International Journal of Engineering Sciences*, VOL. 28, P. 943–957, 1990.
- [DAM 99] DAMIL N., POTIER-FERRY M., NAJAH A., CHARI R., LAHMAM H., *An iterative method based upon Padé approximants*, *Communications in Numerical Methods in Engineering*, VOL. 15, P. 701–708, 1999.
- [DEB 97] DE BOER H., VAN KEULEN F., *Padé approximants applied to a non-linear finite element solution strategy*, *Communications in Numerical Methods in Engineering*, VOL. 13, P. 593–602, 1997.
- [ELH 98] ELHAGE-HUSSEIN A., DAMIL N., POTIER-FERRY M., *An asymptotic numerical algorithm for frictionless contact problems*, *Revue Européenne des Eléments Finis*, VOL. 7, P. 119–130, 1998.
- [ELH 00] ELHAGE-HUSSEIN A., POTIER-FERRY M., DAMIL N., *A numerical continuation method based on Padé approximants*, *International Journal of Solids and Structures*, VOL. 37, P. 6981–7001, 2000.
- [HOF 89] HOFFMANN W., *Iterative algorithm for Gram-Schmidt orthogonalization*, *Computing*, VOL. 41, P. 335–348, 1989.
- [JAM 01] JAMAI R., DAMIL N., *Quadratic approximants in the asymptotic numerical method*, *Comptes Rendus de l'Académie des Sciences, Paris*, VOL. 329, SÉRIE II B, P. 809–814, 2001.
- [JAMA 02] JAMAL M., BRAIKAT B., BOUTMIR S., DAMIL N., POTIER-FERRY M., *A high order implicit algorithm for solving nonlinear problems*, *Computational Mechanics*, VOL. 28, P. 375–390, 2002.
- [JAM 02] JAMAI R., *Contribution des approximants de Padé et des approximants quadratiques dans la Méthode Asymptotique Numérique: Application en calcul des structures*, *Doctorat, Université Hassan II - Mohammedia, Faculté des Sciences Ben M'Sik, Casablanca, Maroc*, 2002.
- [JAM 03] JAMAI R., DAMIL N., *Influence of iterated Gram-Schmidt orthonormalization in the asymptotic numerical method*, *Comptes Rendus Mécanique*, VOL. 331, ISSUE 5, P. 351–356, 2003.

- [LAH 02] LAHMAM H., CADOU J.M., ZAHROUNI H., DAMIL N., POTIER-FERRY M., *High-order predictor-corrector algorithms*, *International Journal for Numerical Method in Engineering*, VOL. 55, p. 685–704, 2002.
- [LIN 00] LINGEN F. J., *Efficient Gram-Schmidt orthonormalization on parallel computers*, *Communications in Numerical Methods in Engineering*, VOL. 16, p. 57–66, 2000.
- [MAL 99] MALLIL E., *Développement d'une méthode itérative basée sur les séries et les approximations de Padé pour le calcul non linéaire des structures*, *Doctorat, Université Hassan II - Mohammedia, Faculté des Sciences Ben M'Sik, Casablanca, Maroc*, 1999.
- [MAL 00] MALLIL E., LAHMAM H., DAMIL N., POTIER-FERRY M., *An iterative process based on homotopy and perturbation techniques*, *Computer Methods in Applied Mechanics and Engineering*, VOL. 190, p. 1845–1858, 2000.
- [NAJ 96] NAJAH A., *Calcul non linéaire des structures par des méthodes asymptotiques numériques et accélération de la convergence*, *Thèse de 3ème cycle, Université Hassan II - Mohammedia, Faculté des Sciences Ben M'Sik, Casablanca, Maroc*, 1996.
- [NAJ 98] NAJAH A., COCHELIN B., DAMIL N., POTIER-FERRY M., *A critical review of asymptotic numerical methods*, *Archives of Computational Methods in Engineering*, VOL. 5, n° 1, p. 31–50, 1998.
- [PAD 92] PADÉ H., *Sur la représentation approchée d'une fonction par des fractions rationnelles*, *Annales de l'Ecole Normale Supérieure, série 3*, VOL. 9, p. 3–93, 1892.
- [SHA 74] SHAFER R.E., *On quadratic approximation*, *SIAM J. Numer. Anal.*, VOL. 11 (2), p. 447–460, 1974.
- [TRI 96] TRI A., COCHELIN B., POTIER-FERRY M., *Résolution des équations de Navier-Stokes et détection des bifurcations stationnaires par une méthode asymptotique numérique*, *Revue Européenne des Eléments Finis*, VOL. 5 (4), p. 415–442, 1996.
- [VAN 84] VAN-DYKE M., *Computed-extended series*, *Annual Review in Fluid Mechanics*, VOL. 16, p. 287–309, 1984.
- [ZAH 98] ZAHROUNI H., ELASMAR H., DAMIL N., POTIER-FERRY M., *Asymptotic numerical method for non-linear constitutive laws*, *Revue Européenne des Eléments Finis*, VOL. 7 (7), p. 841–869, 1998.